Published in final edited form as:
Biochim Biophys Acta. 2014 January ; 1841(1): . doi:10.1016/j.bbalip.2013.08.013.

Loss of β-carotene 15,15′-oxygenase in developing mouse tissues alters esterification of retinol, cholesterol and diacylglycerols

Joseph L. Dixon[1,4,5], **Youn-Kyung Kim**[2,4,5], **Anita Brinker**[3,4], and **Loredana Quadro**[2,4,*]
[1]Department of Nutritional Sciences, Rutgers University, New Brunswick, NJ 08901, USA
[2]Department of Food Science, Rutgers University, New Brunswick, NJ 08901, USA
[3]Institute for Food, Nutrition and Health, Rutgers University, New Brunswick, NJ 08901, USA
[4]Rutgers Center for Lipid Research, Rutgers University, New Brunswick, NJ 08901, USA

Abstract

We provide novel insights into the function(s) of β-carotene-15,15′-oxygenase (CMOI) during embryogenesis. By performing *in vivo* and *in vitro* experiments, we showed that CMOI influences not only lecithin:retinol acyltransferase but also acyl CoA:retinol acyltransferase reaction in the developing tissues at mid-gestation. In addition, LC/MS lipidomics analysis of the CMOI−/− embryos showed reduced levels of four phosphatidylcholine and three phosphatidylethanolamine acyl chain species, and of eight triacylglycerol species with four or more unsaturations and fifty-two or more carbons in the acyl chains. Cholesteryl esters of arachidonate, palmitate, linoleate, and DHA were also reduced to less than 30% of control. Analysis of the fatty acyl CoA species ruled out a loss in fatty acyl CoA synthetase capability. Comparison of acyl species suggested significantly decreased 18:2, 18:3, 20:1, 20:4, or 22:6 acyl chains within the above lipids in CMOI-null embryos. Furthermore, *LCAT*, *ACAT1 and DGAT2* mRNA levels were also downregulated in CMOI−/− embryos. These data strongly support the notion that, in addition to cleaving β-carotene to generate retinoids, CMOI serves an additional function(s) in retinoid and lipid metabolism and point to its role in the formation of specific lipids, possibly for use in nervous system tissue.

Keywords

β-carotene; β-carotene cleavage enzyme; acylation reaction; gene expression

1. INTRODUCTION

The carotenoid β-carotene (bC) is the most abundant and best characterized precursor of vitamin A, an essential nutrient for the developing embryo [1]. Conversion of bC into retinoids (vitamin A and its derivatives) occurs by means of two possible mechanisms: 1.

*Corresponding author: Department of Food Science and Rutgers Center for Lipid Research, Rutgers University, New Brunswick, NJ, 08901, Tel. +1 848 932 5491, Fax +1 732 932 6776; quadro@aesop.rutgers.edu.
[5]These authors contributed equally to the work

symmetric cleavage of bC at the 15–15′ carbon-carbon double bond mediated by the enzyme β-carotene-15,15′-oxygenase (CMOI) to potentially give rise to two molecules of retinal (vitamin A aldehyde) from which all other retinoids can be synthesized through the action of endogenous enzymes [2]; 2. asymmetric cleavage of bC to generate a β-ionone ring and apocarotenals, which in turn can produce one molecule of retinal upon chain shortening [2]. To date, β-carotene-9′,10′-oxygenase (CMOII) is the only known enzyme with bC asymmetric cleavage properties [2, 3].

Loss of CMOI function studies in mice have unequivocally confirmed that this is the primary enzyme that generates retinoids from bC in adult mammalian tissues. Indeed, when fed a diet containing 1 mg/g bC but no preformed vitamin A, CMOI−/− mice accumulate large amounts of intact bC in serum, liver, adipose and intestine, and correspondingly retinoid levels are reduced in several tissues known to express CMOI (lung, testis, uterus) [4]. Interestingly, regardless of the vitamin A content of the diet, CMOI−/− mice accumulate lipids in serum and liver, and show altered hepatic expression of genes involved in fatty acid metabolism, as well as increased mRNA levels of PPARγ-activated genes in visceral adipose tissue [4]. Also, CMOI−/− mice are more susceptible to diet-induced obesity and develop a more severe fatty liver phenotype accompanied by increased levels of serum free fatty acids and cholesteryl esters when maintained on a high-fat diet [4]. Further *in vitro* studies support the hypothesis that bC conversion to retinoids, likely retinal and retinoic acid, *via* CMOI may influence lipid metabolism in adipocytes by modulating PPARγ and RAR signaling pathways [5, 6]. Nevertheless, it is still not clear whether CMOI affects lipid metabolism in various tissues in a similar manner and/or independent of its ability to cleave bC. Overall, the molecular mechanisms underlying the apparent ability of CMOI to modulate lipid metabolism have not been fully elucidated.

Our laboratory has demonstrated the importance of bC in supporting mammalian embryonic development by showing *in vivo* the ability of intact bC circulating in the maternal bloodstream to cross the placenta toward the fetus, as well as the ability of embryonic CMOI to generate locally, i.e. in the developing tissues, retinoids from bC [7]. These studies also provided evidence for a potential novel role of CMOI, independent of its major known function of bC cleavage, since bC was not present in the diet (or tissues) of our experimental animals, unless supplemented. Specifically, we showed that lack of this enzyme in the embryo reduced lecithin:retinol acyltransferase (LRAT) mRNA expression and activity, thus impairing retinyl ester formation [7].

In the attempt to gain further insights into the molecular mechanisms of this alternative function of the bC cleavage enzyme, we performed *in vitro* and *in vivo* experiments demonstrating that an acyl CoA:retinol acyltransferase activity exists in mouse embryo at mid-gestation and that this activity is nearly abolished in the CMOI−/− strain. These data argue in favor of CMOI influencing the above-mentioned enzymatic reaction in the developing tissues. We also showed that the embryonic lipid profile is altered in the absence of CMOI. Specifically, the concentrations of a subset of acyl species in phospholipids, triacylglycerols, and cholesteryl esters were significantly reduced. Acyl CoAs and free cholesterol were not different between embryos of the two genotypes. Furthermore, we demonstrated a concomitant downregulation of mRNA expression levels of *LCAT* and *ACAT1*, two of the three enzymes known to esterify cholesterol [8, 9], as well as of DGAT2, one of the two enzymes that catalyze the formation of triacylglycerols from diacylglycerol and acyl CoAs (Reviewed in [10]). All together, these data indicate that, in addition to cleaving intact bC, embryonic CMOI may influence, through multiple mechanisms, the pools of fatty acyl esters that are formed from retinol, cholesterol and diacylglycerol.

2. MATERIALS AND METHODS

2.1 Reagents

All solvents for analytical determinations were HPLC grade. Tetrahydrofuran, 2,2,4-trimethylpentane, toluene, and isopropanol were from J.T. Baker (Avantor Performance Materials Inc., Center Valley, PA); acetone and water were from EMD Chemicals, Inc. (Gibbstown, NJ). Heptadecanoyl CoA and trimyristin were purchased from Sigma (St. Louis, MO); oleoyl CoA and the phospholipid standards were purchased from Avanti Polar Lipids, Inc. (Alabaster, AL); the other triacylglycerol standards and cholesteryl oleate were purchased from Nu-Chek Prep, Inc. (Elysian, MN). Acetonitrile, methylene chloride, and methanol were from Fisher Scientific (Pittsburgh, PA); retinol, retinyl palmitate, retinyl acetate, and β-carotene were purchased from Sigma (St. Louis, MO); echinenone was purchased from Carotenature (Switzerland).

2.2 Animals

Wild-type, CMOI knockout mice (CMOI−/−; [4]) and mice lacking both LRAT and CMOI (LRAT−/−CMOI−/−) were used for our studies. All mice employed in this study were from a mixed genetic background C57BL/6 × 129sv. LRAT−/−CMOI−/− mice were generated by crossing LRAT−/− [11] and CMOI−/− [4] mice. The resulting double heterozygous mice (LRAT+/− CMOI+/−) of the F1 generation were crossed, and the double knock-out animals (LRAT−/−CMOI−/−) were obtained in the F2 generation at the expected Mendelian ratio. The LRAT and the CMOI genotype were confirmed by PCR analysis following published procedures [7, 11]. When maintained on regular chow diet, LRAT−/−CMOI−/− mice were viable and fertile and did not show any obvious phenotype. For all the studies both diet and water were available to the animals on an *ad libitum* basis. Mice were maintained on a 12:12 light/dark cycle with the period of darkness between 7 PM and 7 AM. All experiments were conducted in accordance with the National Institutes of Health Guide for the Care and Use of Laboratory Animals [12] and were approved by the Rutgers University Institutional Committee on Animal Care.

Wild-type, CMOI−/− and LRAT−/−CMOI−/− mice were maintained throughout life and gestation on a standard nutritionally complete regular chow diet (Prolab Isopro RMH3000 5p7, energy from protein, fat and carbohydrates, 26%, 14% and 60%, respectively; vitamin A, 29 IU/g of diet; bC, from trace to 2.6 ppm) manufactured by LabDiet (W.F. Fisher and Son, Inc., NJ). Three-month old female mice were mated with males of the respective genotype. The time of vaginal plug detection was set as 0.5 days *post coitum* (dpc), the onset of gestation. At 14.5 dpc the dams were euthanized by CO_2 inhalation between the hours of 9 AM and 11 AM. Maternal serum and liver as well as embryos were collected, frozen and stored at −80°C until further analyses. Different sets of embryos were used to measure retinoids and bC levels by HPLC, lipids by LC-MS and to perform QPCR analysis.

2.3 Retinol, retinyl ester and bC analysis by HPLC

Reverse-phase HPLC analysis was performed to measure serum and tissue retinoid levels [13] and bC levels [7]. Tissues (100–200 mg) were homogenized in PBS using a PRO200 homogenizer (Oxford, CT). Half of the homogenate was used to extract retinoids [13]. The other half was used to extract bC by adding 0.5 ml of methanol and 1 ml of acetone, and then performing the extraction with 1 ml of petroleum ether. This latter extraction was repeated twice and the supernatant was treated as for retinoid analysis. Retinoids and bC were separated on a 4.6 × 250 mm Ultrasphere C18 column (Beckman, Fullerton, CA) preceded by a C18 guard column (Supelco Inc., Bellefonte, PA) using acetonitrile, methanol, and methylene chloride (70:15:15, v/v) as the mobile phase flowing at 1.8 ml/min. A Dionex (Sunnyvale, CA) Ultimate 3000 HPLC system with a diode array detector and a

computerized data analysis workstation with Chromeleon software were used. Retinol, retinyl esters and bC were identified by comparing retention times and spectral data of experimental compounds with those of authentic standards. Retinyl acetate (for retinoids) and echinenone (for bC) were added as internal standards. Detection limits were as follows: for retinoids - serum <0.1 ng/dl and tissues <1 ng/g; for bC – serum <1 ng/dl and tissues 10 ng/g.

2.4 Lipid analysis by LC/MS

2.4.1 Measurement of triacylglycerols and phospholipids—Neutral and polar lipids were measured by normal phase HPLC coupled to mass spectrometry, a method pioneered by several investigators. Sommer et al. [14] greatly advanced the normal phase HPLC/electrospray ionization/mass spectrometry method by adding ammonium ions directly to the solvents for polar lipids or post-column using a pump and T-fitting for non-polar lipids. This method was adapted by Hermansson et al. [15] and Brown and colleagues [16, 17] to measure polar lipids in cells, and by Hutchins et al. [18] to measure cholesteryl esters, triacylglycerols, and diacylglycerols in RAW 264.7 macrophage cells. Lipid extracts (Folch) were evaporated to dryness under a nitrogen stream and re-dissolved in isooctane/tetrahydrofuran (9:1, v/v). The lipids were measured in a single chromatographic run without pre-separation, using a Dionex UltiMate 3000 LC system coupled to an Applied Biosystems 4000 QTrap mass spectrometer with a Turbo V electrospray ionization source (ABSciex, Foster City, CA). The high performance liquid chromatography column was a Spherisorb® S5W 4.6 × 100 mm silica cartridge, 5 μm particle size, with a Spherisorb® S5W 4.6 × 10 mm guard cartridge (Waters, Milford, MA). The tertiary normal phase chromatography utilized here was pioneered by Christie [19] and later modified by Homan and Anderson [20]. The solvents were: A = isooctane:tetrahydrofuran (99:1), B = isopropanol:acetone (2:1), C = isopropanol:water (85:15). The gradient was: 0 min, A = 100%; 1 min, A = 100%; 8 min, A = 96%, B = 4 %; 10 min, A = 95%, B = 5 %; 12 min, A = 95%, B = 5 %; 15 min, A = 70%, B = 30 %; 15.1 min, A = 40%, B = 50 %, C = 10%; 26 min, A = 40%, C = 60%; 41 min, A = 40%, C = 60%; 41.5 min, B = 100%; 43.5 min, B = 100%; 44.5 min, A = 100%; 53 min, A = 100%. The flow rate was 1 ml/min. A co-ionization solution (20 mM ammonium formate, 0.01 mM sodium acetate in isopropanol) was delivered post-column through a tee about 10 cm before the inlet to the Turbo V source. The co-ionization solution was delivered at 400 μl/min from 0 to 15 min and at 50 μl/min thereafter. These conditions produced mainly positively charged ammonium ions for triacylglycerol species (which eluted from 6 to 8.8 minutes) and protonated [M+H]+ or negatively charged [M-H]- phospholipid species that eluted thereafter. The full HPLC run from the original Homan gradient was lengthened to 53 min to fully re-equilibrate the column and to remove all lipids from the column before the following run. Each lipid extract was run in duplicate using the same LC gradient but was monitored using two distinct mass spectrometer analysis modes (therefore four injections in total). All runs and standard curves used to quantify triacylglycerols and phospholipids were performed as a single batch. Using the first mode (Mode 1) of analysis, triacylglycerols, PIs, and PSs were analyzed using a wide window Q1 scan from m/z 200 to 1200 as shown in Supplemental Figure 1. Curtain gas setting was 15 (nitrogen was used for all gases with this instrument); source temperature, 450°C; ion voltage, 5000 V; Gas 1, 50; Gas 2, 40; declustering potential, 160; entrance potential, 10; total scan time, 4 seconds; and step size, 0.1 amu. The triacylglycerols peak eluted between 6 and 8.8 minutes and was analyzed using Analyst 1.4.2 software and its companion LipidView software. LipidView was also used to analyze the PI peak at 18.1 minutes. The PI ions ($[M+H]^+$ ions) observed in the Q1 sample runs matched the retention times of the PI standards. Also, the retention times of the major PI ions $[M+H]^+$ observed in the Q1 scan matched (but were offset by 2 amu) those of the PI ions $[M-H]^-$ observed in the spectra obtained using the precursor of m/z 241 scan (in negative mode) used in the second

mode of analysis (see below). PS species were identified in the positive Q1 scans at 21 to 22 minutes using LipidView and were also confirmed using the second mode of analysis.

In the second set of runs (Mode 2), PEs and PCs were analyzed using the spectrometer programmed in three distinct periods as shown in Supplemental Figure 2. In period 1, triacylglycerols were monitored from 0 to 15 minutes using 41 multiple reaction monitoring (MRM scans) ion pairs but we did not use this data in this report as the Q1 scan data was more complete. PEs were monitored in period 2, from 15 to 27 minutes, using a neutral loss of 141 Da scan in positive mode. Conditions for PE were: ion voltage was 5 kV, declustering potential was 90, entrance potential was 10, collision energy was 35, and collision cell exit potential was 11. The other experiments programmed in period 2 were used to confirm the measurements of PIs and PSs made using the Q1 scans. PI was measured with a precursor of m/z 241 scan in negative mode (declustering potential was −190, and collision energy was −65); PS was measured with a neutral loss of 87 Da scan in negative mode (declustering potential was −120, and collision energy was −37). For the latter two experiments in period 2, the entrance potential and collision cell exit potential were −10 and the ion voltage was −4.5 kV; for all three experiments, the collision gas was set to 3, gas 1 was 30, and gas 2 was 35. PCs were monitored in period 3, from 27 to 53 minutes, using precursor of m/z 184 scan in positive mode. The collision gas was set to 2, ion voltage was 5 kV, gas 1 was 30, gas 2 was 40, declustering potential was 120, entrance potential was 10, collision energy was 40, and collision cell exit potential was 15.

2.4.2 Determination of mass amounts for lipid sub-classes—Since lipid sub-classes eluted as distinct peaks that contained all species within a sub-class, the mass of a lipid class could be measured by analysis of the total ion currents using Analyst 1.4.2 software (ABSciex). Internal standards used were trinonanoin and dimyristoyl-PC. Triacylglycerol concentrations were adjusted for the internal standard and estimated from a standard curve containing ten triacylglycerol standards (trinonanoin, trilaurin, tripentadecanoin, triolein, tritridecanoin, tripalmitolein, trilinolein, tripalmitin, tristearin, and trimyristin). The standard curve mixture used for quantification of phospholipids included at least one compound from each class. The compounds used were: dioleoyl-PC, dimyristoyl-PC, dieicosenoyl-PC, and dioleoyl-PE. For PI, a mixture extracted from liver (Avanti Polar Lipids, Alabama) was used for the standard curve. The standard curves were generated for each analysis mode using the exact scan conditions used for the samples.

2.4.3 Determination of lipid species within sub-classes—After the total lipid concentration was determined, the following strategy was used for analysis of lipids using LipidView software. In Mode 1, which used Q1 scans, triacylglycerols eluted between 6 and 8.8 minutes and the Q1 scans were analyzed using LipidView. 1% filtering was the most important LipidView parameter used for triacylglycerol species determination. LipidView identified a total of 47 triacylglycerols (mostly ammonium adducts and a smaller number of sodium adducts) in the samples. Signals from 5 blank runs were averaged and then subtracted from the signals of individual triacylglycerol molecules for each sample. 30 triacylglycerol molecules remained in the analysis pool. The fraction that each of these 30 triacylglycerol species represented out of the whole was multiplied by the calculated total mass of triacylglycerols determined using the standard curve. This allowed for the determination of the concentration of each triacylglycerol species. A similar strategy was used for the other lipids, except for PS, for which there was no standard included and therefore only peak area signals are presented. For PCs, the spectra were analyzed using LipidView using a filter of 0.5% as there were essentially no signals in the blanks. Only very low concentrations of sphingomyelins were observed in embryos (not shown). PEs were also filtered at 0.5%. All ions identified using LipidView were confirmed by direct inspection of the spectra derived from original chromatograms.

2.4.4 Measurement of free cholesterol and cholesteryl esters—We measured the effects of CMO1 loss on the cholesteryl esters in embryos using LC/MS with the normal phase chromatographic method described above and atmospheric pressure photoionization (APPI), which is more sensitive than electrospray ionization for this sub-class under our chromatography conditions. However, this approach results in in-source fragmentation of the esters, so cholesterol and acyl chain fragments are observed rather than the intact cholesteryl esters. The cholesteryl moiety, and also free cholesterol, was measured using the MRM pair *m/z* 369/161; the acyl chains were detected using a Q3 scan in negative mode covering *m/z* 150–350. Throughout the run, the curtain gas was set to 15, gas 1 to 40, gas 2 to 20, and the collision gas to 4. The ion source temperature was 350°C. Toluene was used as the co-infusion dopant. Cholesteryl esters elute at about 1.6 minutes; for the cholesteryl fragment MRM scan during this section of the gradient, the electrode voltage was 950V, the declustering potential was 60, the entrance potential was 6, the collision energy was 33, and the collision cell exit potential was 10. The parallel scan for detection of the acyl chains used the following settings: the electrode voltage was −1.3kV, the declustering potential was −90, the entrance potential was −10, and the collision cell exit potential was −12. Summing the individual fatty acyl species or using the ion formed from the cholesterol portion of the cholesteryl ester molecule both provided similar values for the total concentrations of cholesteryl esters in embryos. Free cholesterol elutes at 7.7 minutes; in this period the electrode voltage was 1100V, the declustering potential was 125, the collision energy was 31, the entrance potential was 10, and the collision cell exit potential was 9. Quantification was based on standard curves of cholesteryl oleate and cholesterol (concentrations 1–60 ng/injection).

2.4.5 Measurement of fatty acyl CoA species—The method used is a combination of two methods [21, 22]. Embryos (150 – 200 mg) were homogenized in 200 μl KH2PO4/K2HPO4 buffer (0.1 M, pH 5.3)/isopropanol (1:1, vol:vol). A small aliquot was taken for protein assay. Heptadecanoyl CoA (C17 acyl CoA, 10 μl of 5.0 μM in methanol:chloroform (2:1)) was added as internal standard. Saturated $(NH_4)_2SO_4$ in water was added at 30 μl/ml homogenate. Acetonitrile (1 vol of homogenate) was then added. The homogenate was vortexed and centrifuged at 6,000 g for 5–10 min at room temperature. The clear upper phase was transferred to LC-MS vials with 400 μl inserts. Extracts were analyzed for fatty acyl CoAs on the same day the homogenates were prepared, using the chromatography method described in Haynes et al. [22]. The LC and MS instruments were those used previously. The column was a Gemini C_{18} column (2 mm ID × 150 mm, 5 μm particle size, Phenomenex, Torrance, CA) with a Gemini 2 × 4 mm guard column with the same packing. The column oven was kept at 40°C and the autosampler at 4°C. Solvent A was water and solvent B was acetonitrile, each with 0.05% (v/v) triethylamine; the flow rate was 0.2 ml/min. The solvent gradient was as follows: 85%A for 5 min, linear ramp to 47.5%A over 14 minutes, linear ramp to 10%A in 1 min, hold for 5 min, return to 85%A in 1 min, re-equilibrate for 5 min. The scan used was a neutral loss of 507 Da in positive mode, to detect all fatty acyl CoAs between *m/z* 900 and 1200. The curtain gas setting was 20, the collision gas was 4, and gas 1 and 2 were both 40. The electrode voltage was 5.5 kV, and the source temperature was 650°C. The declustering potential setting was 155, the entrance potential was 10, the collision energy was 55, and the collision cell exit potential was 9. The standards for the standard curve were the C17 and oleoyl acyl CoAs in methanol:chloroform (2:1). A new standard curve was made every 2 days from the 50 μM methanol:chloroform stocks (stored at −80 °C). A preliminary experiment demonstrated that fatty acyl CoAs were stable in embryos stored at −80 °C.

2.5 RNA extraction, cDNA synthesis, and quantitative real-time PCR (QPCR)

Total embryonic RNA was extracted using the RNA Bee kit (Tel-test Inc, TX) according to the manufacturer's instructions. RNA concentrations were measured by using the Nanodrop Spectrophotometer ND-1000 (Nanodrop Technologies, DE) and quality was ascertained by 260/280 ratio and by a formaldehyde gel. This step was followed by DNase I treatment (Roche Diagnostics, IN). One microgram of the DNase-treated RNA was reverse transcribed to cDNA using the instructions and reagents (random hexamer primers were used) from Transcriptor First Strand cDNA Synthesis kit (Roche Diagnostics, IN) in a final volume of 20 μl. A no-reverse transcriptase control (NRTC) was included. The LightCycler 480 SYBR Green I Master kit (Roche Diagnostics, IN) was used for QPCR. A validation test (calibration curve) was carried out for each primer pair using a pool of control samples to determine PCR efficiency. Reactions were performed according to the protocol of the manufacturer with 300 nmol/L of each primer (final concentration), cDNA and the SYBR Green I. All the analyzed amplicons of the genes of interest encompass at least one intron. For the QPCR experiments, 300 nmol/L of each primer (final concentration), together with an amount of cDNA for each sample equivalent to 10–20 ng of the total RNA input in a final volume of 15 μl was used. Primer sequences were as follows: *LCAT*, Fwd 5′GGATATGTGCGGGATGAGAC3′, Rev 5′AGTGGAGCACATGCAGACAG3′; *ACAT1*, Fwd 5′AGCCCAGAGGCTCAATGTTA3′, Rev 5′GGCTAGCACAACCACACTGA3′; *ACAT2*, Fwd 5′TGTCACAGAACAGGGCAGAG3′, Rev 5′TGACAGTTCCTGTCCCATCA3′; *DGAT1*, Fwd 5′GCTTCTGCAGTTTGGAGACC3′ Rev 5′CTCATGGAAGAAGGCTGAGG3′; *DGAT2*, Fwd 5′ACGCAGTCACCCTGAAGAAC3′, Rev 5′AGGGGGCGAAACCAATATAC3; *β-ACTIN*, Fwd 5′AACACAGTGCTGTCTGGTGG3′; Rev 5′GAAAGGGTGTAAAACGCAGC 3′. Clear plates were used for the reaction in the Lightcycler 480 machine (Roche Diagnostics, IN). All samples were run in triplicate. Included within each experiment were the NRTC and the non-template control. After enzyme activation (10 min, 95°C), 35–40 PCR amplification cycles were performed: 10 s at 95°C, 20 s at 60°C, and 30 s at 72°C. At the end of each run, samples were heated to 95°C with a temperature transition rate of 0.11°C/s to construct dissociation curves. For each gene, several samples were tested on a 2% agarose gel. Both the reverse transcription and QPCR steps were repeated twice.

From the instrument, cycle thresholds (Ct) were obtained for each sample for each gene of interest. To determine changes in gene expression, the ΔΔCt method was used. Briefly, ΔCt values were obtained for each sample by subtracting the Ct of the gene of interest from that of the housekeeping gene. The ΔΔCt values were obtained from subtracting ΔCt for each sample from the average ΔCt for the calibrator group (WT). The expression of each gene relative to the calibrator was calculated using $2^{(-\Delta\Delta Ct)}$. All groups were expressed as fold change of the control group (WT).

2.6 Preparation of embryonic microsomes and LRAT enzymatic activity assay

Microsomes were isolated from 2 embryos (0.4 g) by differential centrifugation. Tissues were homogenized in 4 ml of 50 mM potassium phosphate buffer (pH 7.25) containing 25% sucrose and 1mM dithiothreitol (DTT), and centrifuged at 12,000 g for 30 min. Supernatants were centrifuged at 100,000 g for 1 h. All the steps were performed at 4°C. Next, pellets were re-suspended in 100 ul of the homogenization buffer without sucrose and stored at −80°C until further use. Prior to performing the LRAT activity assay, optimal reaction time and concentration of microsomal proteins were determined. For each genotype, 2 microsome preparations (each from 2–3 embryos from different dams) were pooled to be assayed and the experiment was repeated three times. Assay conditions were as follows: 50 ug of microsomal proteins was incubated for 12 min at 37°C with 40 nM [^{3}H]-retinol dissolved in

1mM dimethylformamide (DMF) in 50 mM potassium phosphate buffer (pH 7.25) containing 20 uM fatty acid free bovine serum albumin (BSA) and 1mM DTT. Enzymatic reaction was stopped by adding an equal volume of ice-cold ethanol containing 0.1 mg/ml butylated hydroxytoluene (BHT). As a control, ethanol-BHT was mixed with microsomes before adding the reaction mix. Microsome preparations were assayed with and without phenylmethanesulfonyl fluoride (PMSF), the serine protease inhibitor that selectively inhibits LRAT activity [23, 24]. PMSF was added to the reaction mix at 3mM final concentration. Radiolabeled retinoids were analyzed by HPLC [13], and for each run, the peak corresponding to retinyl palmitate was collected, dried, and mixed with scintillation solution. Note that retinyl esters synthesized by LRAT activity in embryonic microsomes were below the detection limit of the HPLC. Hence, a radioactive tracer ([^{3}H]-retinol) was used to increase the sensitivity of the detection of the reaction product ([^{3}H]-retinyl ester) upon separation of the various retinoids by HPLC and collection of the corresponding fractions.

2.7 Statistical Analyses

Normality of variables was assessed by the Shapiro-Wilk test. Normally distributed data were analyzed by Student's *t*-test or ANOVA. Not normally distributed values were analyzed by Kruskal-Wallis or Mann-Whitney test. A p-value <0.05 was used to establish statistical significance.

3. RESULTS

3.1 CMOI impacts on retinyl ester formation in the developing tissues

Retinoids and bC levels were measured by reverse phase HPLC in embryos from wild-type and CMOI−/− mice at 14.5 days *post-coitum* (dpc) (mid-gestation). As previously reported [7], embryonic retinyl ester but not retinol levels were significantly reduced in the absence of CMOI (retinol: 88.6 ± 3.0 ng/g vs. 96.3 ± 9.4 ng/g; retinyl ester: 205.2 ± 50.3 vs. 103.8 ± 21.7 ng/g, wild-type vs. CMOI−/−, $p < 0.05$ for retinyl ester), while intact bC was undetectable in all the tissues analyzed from these mice (data not shown and [7]). These reduced retinyl ester levels correlate with an attenuated enzymatic activity of LRAT [7], the main enzyme that esterifies retinol [25].

To gain further insights into the possible mechanisms behind the reduction of embryonic retinyl ester content upon loss of CMOI, we tested the retinol acyltransferase activity of wild-type and CMOI−/− microsomes from embryos at mid-gestation, in the presence of phenylmethanesulfonyl fluoride (PMSF), the serine protease inhibitor which selectively inhibits LRAT [23, 24]. As shown in Figure 1, we confirmed the previously reported reduction of LRAT activity in the absence of CMOI [7]. Moreover, the residual enzymatic activity upon PMSF treatment was about 15% in the wild-type strain and nearly abolished in CMOI−/− embryos. We interpret these data as a strong indication that an additional retinol acyltransferase activity exists in the developing tissues, and that this could be an acyl CoA-dependent reaction, as previously described in adult tissues [26]. However, this PMSF-insensitive activity was negligible in the absence of CMOI (Figure 1). Note that addition of PMSF to microsome preparations from wild-type liver, an organ where retinyl ester synthesis is carried out exclusively by LRAT [25], also resulted in extremely low levels of PMSF-insensitive activity, similar to those of CMOI−/− microsomes treated with PMSF (data not shown).

Furthermore, we generated mice lacking both LRAT and CMOI (LRAT−/−CMOI−/−) and compared their embryonic retinyl ester levels with those of wild-type, CMOI−/− and LRAT −/− embryos, at 14.5 dpc. In agreement with the *in vitro* data shown above, LRAT−/− and

CMOI−/− embryos possessed about 8% and 50% of the wild-type embryonic retinyl ester levels, respectively (Table 1), while retinyl ester levels fell below the limit of detection in LRAT−/−CMOI−/− embryos (Table 1). Thus, we propose that in the developing tissues this acyltransferase activity could be facilitated by CMOI.

3.2 Loss of CMOI in the developing tissues alters the concentrations of subsets of lipid acyl species

To establish whether the disruption in acyl CoA transferase capability in embryos lacking CMOI was limited to retinyl ester formation or more broadly impacted pathways leading to the acylation of a range of lipid classes, wild-type and CMOI−/− embryos underwent targeted LC/MS lipidomic analysis to measure masses and species distribution of several sub-classes of lipids. As shown in Figure 2A and 2B, significant reductions in certain species of PCs and PEs with higher degrees of unsaturation were observed in embryos lacking CMOI. Although the PI and PS groups contained two species each that were significantly different between the two strains analyzed, the percent differences were extremely small (Figure 2C and 2D). Although total concentrations of triacylglycerol in CMOI−/− embryos were not different compared to wild-type (21.5 ± 5.5 *vs.* 15.5 ± 3.6 nmol/mg, wild-type *vs.* CMOI−/−; n=4; $p>0.05$), several species of triacylglycerols, in most cases with more than four unsaturations and with total acyl carbons of fifty-two or more, were significantly decreased in the null-embryos (Figure 3). In addition, lack of CMOI significantly reduced the concentration of cholesteryl esters, particularly those with arachidonate, DHA, palmitate, and linoleate acyl chains (Table 2). Cholesteryl oleate, the cholesteryl ester with the highest concentration, was decreased to 68.6% of control. The concentrations and distribution of fatty acyl CoAs, the major substrates for most acylation reactions, were not altered by loss of embryonic CMOI (Figure 4). Similarly, embryonic free cholesterol levels were not different between the two strains (29.0 ± 4.0 ng/μg protein and 26.0 ± 5.2 ng/μg protein in wild-type and CMOI−/− embryos, respectively).

Overall, these data suggest that embryonic CMOI may contribute to the maintenance of the pool of esters derived from retinol, cholesterol and diacylglycerol.

3.3 Loss of CMOI in the developing tissues attenuates mRNA levels of *ACAT1*, *LCAT and DGAT2*

Since lack of CMOI in the developing tissues not only downregulated LRAT activity, but also its mRNA levels [7], we performed a QPCR analysis to establish whether CMOI could exert a similar action on the transcription of acyl CoA:cholesterol acyltransferases (ACATs, specifically ACAT1 and 2) and lecithin:cholesterol acyltransferases (LCAT), the enzymes that synthesize cholesteryl ester [8, 9], as well as on the transcription of acyl CoA:diacylglycerol acyltransferase (DGAT) enzymes (DGAT 1 and 2), which catalyze the final step in the biosynthesis of triacylglycerols [10]. As shown in Figure 5, mRNA levels of *ACAT1* and *LCAT*, but not *ACAT2* were significantly reduced in CMOI−/− embryos compared to wild-type. Also, while mRNA levels of *DGAT1* remained unchanged, those of *DGAT2* were significantly reduced in the null-embryos (Figure 5). Therefore, these findings indicate that in developing tissues, CMOI may also influence the transcription of *ACAT1*, *LCAT* and *DGAT2* similarly to what we previously reported for *LRAT* [7].

4. DISCUSSION

This study aims at furthering our understanding of the role played by CMOI in the developing tissues and builds on previously published data from our laboratory showing that, in addition to its ability to generate retinoids from β-carotene, CMOI influences retinyl ester formation [7]. Work from our laboratory has shown that the mouse embryo at mid-

gestation (E14.5), when the majority of the organogenesis is completed [27], is "metabolically" active and capable of regulating its own retinoid and carotenoid metabolism [1, 7, 28, 29]. For this reason, and for consistency with previous studies from our laboratory, we chose to maintain the focus of the current investigation on this same stage of development.

Tissue retinyl ester stores are synthesized predominantly through the action of lecithin:retinol acyltransferase (LRAT), that catalyzes the transesterification of retinol employing a fatty acyl group present in the A1 position of a membrane phosphatidyl choline molecule [25]. We confirmed that LRAT enzymatic activity was reduced in CMOI−/− embryonic microsomes compared to wild-type, and we interpreted this reduction as the effect of the attenuation of LRAT transcription that also occurs in the absence of CMOI in the developing tissues [7]. Interestingly, when LRAT enzymatic activity was knocked down, either *in vitro* with phenylmethanesulfonyl fluoride (PMSF) [23, 24] or *in vivo* in the LRAT −/− embryos, retinyl ester formation was not fully abolished (Figure 1 and Table 1), indicating that an additional retinol acyltransferase activity may exist in the developing tissues. This activity contributes to about 10–15% of the total retinyl ester formed in the mouse embryo at mid-gestation. Earlier studies have suggested that an unidentified acyl CoA:retinol acyltransferase (ARAT), catalyzing the fatty acyl CoA-dependent esterification of retinol, may work in conjunction with LRAT to synthesize retinyl ester [30]. However, the genetic identity of such an enzyme has been unraveled only in certain adult tissues. In the mouse intestine, for example, the enzyme diacylglycerol acyltransferase 1 (DGAT1), which catalyzes triglyceride synthesis from diacylglycerol and fatty acyl CoA, acts as a physiologically significant ARAT, accounting for approximately 10% of the retinol esterified in this tissue under physiological conditions [26]. Accordingly, retinyl esters were undetectable in chylomicrons isolated from LRAT/DGAT1-double knockout mice given a physiologic dose of retinol [26]. Here we show that CMOI may influence retinyl ester formation also by facilitating another retinol esterification reaction that is likely acyl CoA-dependent. Indeed, when LRAT is either pharmacologically (PMSF) or genetically (LRAT −/−) inhibited, the residual embryonic retinol acyltransferase activity is negligible *in vitro* (Figure 1) and completely abolished *in vivo* (Table 1) in the absence of CMOI. Therefore, at least when the mice were maintained on a vitamin A sufficient diet, DGAT1 did not seem to contribute significantly to embryonic retinyl ester synthesis. However, we cannot completely rule out that, as demonstrated in the case of small intestine, a second ARAT activity, may contribute towards retinyl ester formation under non-physiological conditions of vitamin A intake, for example [26]. In this case, DGAT1, which has been suggested to contribute to hepatic retinyl ester synthesis when cellular retinol concentrations were relatively high [31], could be the enzyme responsible for such additional ARAT activity. This possibility, however, remains to be confirmed. Overall, our data strongly support the possibility that embryonic CMOI may influence retinyl ester formation rather than turnover, specifically facilitating an acyl CoA-dependent retinol esterification.

As highlighted in the introduction, a role for CMOI in regulating lipid homeostasis in adult tissues has been proposed [4] [5, 6]. However, the molecular mechanisms underlying the ability of CMOI to modulate lipid metabolism have not been fully elucidated and it is certainly not known whether they may be tissue-specific. Here we show that the lipid profile was altered in the absence of CMOI in the embryos from dams maintained on a regular chow diet. Indeed, the concentrations of specific lipid sub-classes were significantly reduced. These included certain species of phospholipids, triacylglycerols, and all the cholesteryl esters measured (Figure 2, Figure 3 and Table 2). This reduction, however, was not due to impaired formation of fatty acyl CoAs, the major substrates for most acylation reactions [32], as embryonic fatty acyl CoAs concentrations and distribution were not altered by loss of CMOI (Figure 4). Also, the reduction in cholesteryl ester was not due to

reduced levels of free cholesterol, the other substrate for cholesteryl ester synthesis [32]. Comparison of all the fatty acids in the lipid sub-classes that were significantly decreased in CMOI−/− embryos shows a consistent and interesting structural pattern (Table 3). The four PCs and three PEs that were decreased in the embryos in the absence of CMOI (64–68% and 70–82% of wild-type, respectively) likely contain at least one 18:2, 18:3, 20:1, 20:4, or 22:6 fatty acid. A similar observation can be made for the eight triacylglycerol species that were different between wild-type and CMOI−/− embryos. Finally, the cholesteryl esters that were most strongly decreased were esters of 20:4, 22:6, 16:0, and 18:2 fatty acids (Table 3). One could make several observations from these data. First, the modest decreases in the cholesteryl esters of 18:0, 18:1, and 16:1 are possibly due to a decrease in ACAT activity, as these are important substrates for this enzyme [32]. Specificity of ACAT for acyl CoA substrates is difficult to determine due to the insolubility of ACAT protein. When ACAT1 and ACAT2 cDNAs were expressed in cells, they were found to have fairly broad acyl CoA specificities [32]. Earlier studies indicated that oleoyl-CoA produced the highest activity for ACAT in liver [33]. In mouse liver, the predominant cholesteryl esters were esters with 18:1 (60–65%) and 16:0 (7–9%) fatty acids when mice were fed diets containing either saturated or monounsaturated fat, respectively [34]. In our studies, similar to mouse liver, mouse embryos contained cholesteryl oleate and palmitate as the 2 major cholesteryl esters (Table 2). Second, the very large decreases in the cholesteryl esters of 20:4, 22:6, and 18:2 fatty acids may be due to a combination of a decrease in ACAT and another putative protein involved, for example, in acyl transfer or trafficking. Interestingly, there has been a report that acyl CoA binding protein stimulated microsomal ACAT activity 3–8 fold when exogenous cholesterol was present [35]. Finally, from comparing the lipid species that were significantly decreased across three major sub-classes (Table 3), it appears that the putative protein affected in CMOI−/− embryos could be a protein that has a high specificity for 18:2, 18:3, 20:1, 20:4, or 22:6 fatty acids.

Overall, our data suggest that CMOI, independent of its ability to cleave intact bC (bC was not detectable in the tissues of these mice), may be involved in regulating the retinyl ester pool in the embryo, by facilitating retinol esterification. They also indicate that CMOI may play a similar action in regards to cholesteryl ester, triacylglycerol and even PC and PE synthesis. While the molecular mechanisms are still not fully elucidated, based on the results of our experiments we hypothesize that CMOI influences ester formation from retinol, cholesterol and diacylglycerol by either facilitating fatty acid transport and trafficking or acting itself as an acyltransferase. The absence of the conserved acyltransferase consensus motif HXXXXD [36] in the CMOI protein does not argue in favor of the latter possibility. Nonetheless, we cannot exclude any hypothesis at the moment.

Interestingly, we previously reported that loss of CMOI function studied in an established model of mouse embryonic vitamin A deficiency (VAD), i.e. the retinol-binding protein knockout mice (RBP−/−), exacerbates the severity of VAD and thus the embryonic malformations of mice lacking RBP, the sole specific transport protein for retinol in the bloodstream [37]. In addition to the RBP−/− like phenotype (eye malformations and peripheral edema), embryos from double-knockout dams (CMOI−/−RBP−/−) showed a certain percent of cleft face and palate or exencephaly [7]. It is intriguing that upon maternal bC supplementation of this mouse strain we could improve the severity of these defects with the exception of the excencephaly [7]. The holoprosencephalic phenotype, which is characterized by abnormal development of the forebrain, absence of olfactory apparatus, and abnormalities of facial structures that originate from forebrain-derived neural crest and contiguous mesoderm, has been described in mouse models of VAD [38] and mice bearing retinoid receptor gene disruption [39]. However, this phenotype has also been linked in human and animal studies to insufficient supply of cholesterol during development (Reviewed in [40, 41]). It has been described in genetically modified mice with alterations

in the metabolic pathway(s) that ensure uptake of cholesterol-carrying lipoproteins by the embryonic tissues [42–44]. Also, pharmacological inhibition of 7-dehydrocholesterol-Δ7-reductase, a late enzyme in the cholesterol biosynthetic pathway, has been shown to produce a holoprosencephalic syndrome in rats [45]. It is therefore intriguing to hypothesize that the rescue of the exencephaly in our model system could not be achieved because this is not a vitamin A-dependent but rather a lipid-dependent phenotype, possibly related to the formation of neuronal membranes containing highly unsaturated PCs and PEs.

Our QPCR analysis indicated that, in developing tissues, CMOI also influences the transcription of *ACAT1*, *LCAT*, and *DGAT2* (Figure 5). We postulate that the reduction in the above-mentioned mRNA levels in the absence of CMOI would result in a reduced enzymatic activity of ACAT1, LCAT and DGAT2, similar to what we previously reported about the effect of the lack of CMOI on embryonic LRAT mRNA and activity [7]. It also remains to be established how CMOI, which is not known to be a transcription factor, may regulate the mRNA levels of other genes. CMOI-mediated cleavage of bC will lead to the generation of retinoic acid, which regulates the expression of *LRAT in vivo* [46], and has multiple effects on energy balance and lipid metabolism [47, 48], at least in adult tissues. However, as we previously reported [7], consistent with their normal phenotype, retinoic acid levels of CMOI−/− embryos from dams fed a vitamin A-sufficient diet did not differ from those of wild-type embryos from dams under the same dietary regimen. Moreover, intact bC was undetectable in the tissues of our mice [7]. Thus, we exclude that the transcriptional effect of CMOI could be mediated by retinoic acid. As we previously proposed [7], one possibility could be that, in the absence of (and/or in addition to) bC, CMOI may cleave an alternative substrate(s) thus controlling the generation of signaling molecules that in turn are able to influence, directly or indirectly, the transcription of *ACAT1*, *LCAT*, *DGAT2* and *LRAT*. Alternatively, CMOI, which is a cytoplasmic enzyme [2], may form a complex with other protein(s), carrier(s) of signaling molecules for transcription factor(s) that may have *ACAT1*, *LCAT*, *DGAT2* and *LRAT* as target genes. It is noteworthy that promoter analysis of the above-mentioned genes revealed the presence of *cis*-elements for common transcription factors (data not shown). Experiments are ongoing to address this question.

In summary, this is the first report to suggest that, in addition to cleaving intact bC, embryonic CMOI influences, through multiple mechanisms, the formation of fatty acyl esters derived from retinol, cholesterol and diacylglycerols. On one hand, it may influence the transcription of certain genes, such as *LRAT*, *LCAT*, *ACAT1* and *DGAT2*, thus ultimately affecting the enzymatic activity of the corresponding proteins; and, on the other hand, CMOI may be more directly involved in these acyltransferase reactions itself, acting as a lipid transporter or as an esterification enzyme, for example. To our knowledge, no data have been reported in the literature regarding changes in retinyl ester, cholesteryl ester or triacylglycerol levels in tissues of adult CMOI−/− mice, with the exception of increased serum cholesteryl ester and serum and liver triacylglycerol levels in the CMOI knockout mice maintained on a high-fat diet [4]. Therefore, at the moment this action seems to be restricted to the developing tissues (embryo and yolk sac [7, 29]). The observation that the long chain unsaturated fatty acid moiety of several lipid sub-classes was severely attenuated in the absence of embryonic CMOI points to an important and novel role of this enzyme in the homeostasis of specific lipids that are crucial for embryonic development. Long chain polyunsaturated fatty acids are highly concentrated in the cell membranes of the brain and the retina, where they act as modulators of membrane function [49–51]. The severe abnormalities observed in brain formation with CMOI ablation support this interpretation of the data and suggest that CMOI may facilitate the utilization of these fatty acids by the developing nervous system. Moreover, preliminary experiments from our laboratory indicated reduced mRNA levels of peroxisome proliferator-activated receptors, PPARα and

PPARγ, in embryos lacking CMOI compared to wild-type (data not shown). Since these transcription factors mainly regulate the expression of target genes involved in lipid and energy metabolism [52–54] and are activated by long chain fatty acids and their metabolites [55], our data seem to support the idea that this alternative function of CMOI may have a more profound effect on fatty acid metabolism in the embryo. Overall, these findings add an additional unexpected layer of complexity to the alternative function(s) that CMOI may play in the developing tissues. They also position more clearly the bC cleavage enzyme CMOI at the intersection between lipid and retinoid metabolism.

Supplementary Material

Refer to Web version on PubMed Central for supplementary material.

Acknowledgments

We thank Dr. George Carman and Dr. Gil-Soo Han for their invaluable guidance in performing the enzymatic assays. We also thank Dr. Lesley Wassef and Mrs. Elizabeth Spiegler for helpful comments on the manuscript. This work was supported by grants R01HD057493 and R01HD057493-02S1 from the U.S. National Institute of Health (NIH) to L.Q. The liquid chromatography-mass spectrometry system was obtained through the National Center for Research Resources Grant RR021120 from the NIH.

Abbreviations

bC	β-carotene
CMOI	β-carotene 15,15′-oxygenase
CMOII	β-carotene-9′,10′-oxygenase
PC	phosphatidylcholine
PE	phosphatidylethanolamine
PI	phosphatidylinositol
PS	phosphatidylserine

References

1. Spiegler E, Kim YK, Wassef L, Shete V, Quadro L. Maternal-fetal transfer and metabolism of vitamin A and its precursor beta-carotene in the developing tissues. Biochim Biophys Acta. 2012; 1821:88–98. [PubMed: 21621637]
2. Lobo GP, Amengual J, Palczewski G, Babino D, von Lintig J. Mammalian carotenoid-oxygenases: key players for carotenoid function and homeostasis. Biochim Biophys Acta. 2012; 1821:78–87. [PubMed: 21569862]
3. Kiefer C, Hessel S, Lampert JM, Vogt K, Lederer MO, Breithaupt DE, von Lintig J. Identification and characterization of a mammalian enzyme catalyzing the asymmetric oxidative cleavage of provitamin A. J Biol Chem. 2001; 276:14110–14116. [PubMed: 11278918]
4. Hessel S, Eichinger A, Isken A, Amengual J, Hunzelmann S, Hoeller U, Elste V, Hunziker W, Goralczyk R, Oberhauser V, von Lintig J, Wyss A. CMO1 Deficiency Abolishes Vitamin A Production from beta-Carotene and Alters Lipid Metabolism in Mice. J Biol Chem. 2007; 282:33553–33561. [PubMed: 17855355]
5. Lobo GP, Amengual J, Li HN, Golczak M, Bonet ML, Palczewski K, von Lintig J. Beta, beta-carotene decreases peroxisome proliferator receptor gamma activity and reduces lipid storage capacity of adipocytes in a beta, beta-carotene oxygenase 1-dependent manner. J Biol Chem. 2010; 285:27891–27899. [PubMed: 20573961]
6. Amengual J, Gouranton E, van Helden YG, Hessel S, Ribot J, Kramer E, Kiec-Wilk B, Razny U, Lietz G, Wyss A, Dembinska-Kiec A, Palou A, Keijer J, Landrier JF, Bonet ML, von Lintig J. Beta-

carotene reduces body adiposity of mice via BCMO1. PLoS One. 2011; 6:e20644. [PubMed: 21673813]

7. Kim YK, Wassef L, Chung S, Jiang H, Wyss A, Blaner WS, Quadro L. {beta}-Carotene and its cleavage enzyme {beta}-carotene-15,15′-oxygenase (CMOI) affect retinoid metabolism in developing tissues. FASEB J. 2011; 25:1641–1652. [PubMed: 21285397]
8. Chang TY, Li BL, Chang CC, Urano Y. Acyl-coenzyme A:cholesterol acyltransferases. Am J Physiol Endocrinol Metab. 2009; 297:E1–9. [PubMed: 19141679]
9. Rousset X, Shamburek R, Vaisman B, Amar M, Remaley AT. Lecithin cholesterol acyltransferase: an anti- or pro-atherogenic factor? Curr Atheroscler Rep. 2011; 13:249–256. [PubMed: 21331766]
10. Yen CL, Stone SJ, Koliwad S, Harris C, Farese RV Jr. Thematic review series: glycerolipids. DGAT enzymes and triacylglycerol biosynthesis. J Lipid Res. 2008; 49:2283–2301. [PubMed: 18757836]
11. O'Byrne SM, Wongsiriroj N, Libien J, Vogel S, Goldberg IJ, Baehr W, Palczewski K, Blaner WS. Retinoid absorption and storage is impaired in mice lacking lecithin:retinol acyltransferase (LRAT). J Biol Chem. 2005; 280:35647–35657. [PubMed: 16115871]
12. N.R. Council. Guide for the care and use of laboratory animals. 7. National Academy Press; Washington, D.C: 1996.
13. Kim YK, Quadro L. Reverse-phase high-performance liquid chromatography (HPLC) analysis of retinol and retinyl esters in mouse serum and tissues. Methods Mol Biol. 2010; 652:263–275. [PubMed: 20552434]
14. Sommer U, Herscovitz H, Welty FK, Costello CE. LC-MS-based method for the qualitative and quantitative analysis of complex lipid mixtures. J Lipid Res. 2006; 47:804–814. [PubMed: 16443931]
15. Hermansson M, Uphoff A, Kakela R, Somerharju P. Automated quantitative analysis of complex lipidomes by liquid chromatography/mass spectrometry. Anal Chem. 2005; 77:2166–2175. [PubMed: 15801751]
16. Ivanova PT, Milne SB, Byrne MO, Xiang Y, Brown HA. Glycerophospholipid identification and quantitation by electrospray ionization mass spectrometry. Methods Enzymol. 2007; 432:21–57. [PubMed: 17954212]
17. Myers DS, Ivanova PT, Milne SB, Brown HA. Quantitative analysis of glycerophospholipids by LC-MS: acquisition, data handling, and interpretation. Biochim Biophys Acta. 2011; 1811:748–757. [PubMed: 21683157]
18. Hutchins PM, Barkley RM, Murphy RC. Separation of cellular nonpolar neutral lipids by normal-phase chromatography and analysis by electrospray ionization mass spectrometry. J Lipid Res. 2008; 49:804–813. [PubMed: 18223242]
19. Christie WW. Rapid separation and quantification of lipid classes by high performance liquid chromatography and mass (light-scattering) detection. J Lipid Res. 1985; 26:507–512. [PubMed: 4009068]
20. Homan R, Anderson MK. Rapid separation and quantitation of combined neutral and polar lipid classes by high-performance liquid chromatography and evaporative light-scattering mass detection. J Chromatogr B Biomed Sci Appl. 1998; 708:21–26. [PubMed: 9653942]
21. Clugston RD, Jiang H, Lee MX, Piantedosi R, Yuen JJ, Ramakrishnan R, Lewis MJ, Gottesman ME, Huang LS, Goldberg IJ, Berk PD, Blaner WS. Altered hepatic lipid metabolism in C57BL/6 mice fed alcohol: a targeted lipidomic and gene expression study. J Lipid Res. 2011; 52:2021–2031. [PubMed: 21856784]
22. Haynes CA, Allegood JC, Sims K, Wang EW, Sullards MC, Merrill AH Jr. Quantitation of fatty acyl-coenzyme As in mammalian cells by liquid chromatography-electrospray ionization tandem mass spectrometry. J Lipid Res. 2008; 49:1113–1125. [PubMed: 18287618]
23. Fortuna VA, Trugo LC, Borojevic R. Acyl-CoA: retinol acyltransferase (ARAT) and lecithin:retinol acyltransferase (LRAT) activation during the lipocyte phenotype induction in hepatic stellate cells. J Nutr Biochem. 2001; 12:610–621. [PubMed: 12031254]
24. Shingleton JL, Skinner MK, Ong DE. Retinol esterification in Sertoli cells by lecithin-retinol acyltransferase. Biochemistry. 1989; 28:9647–9653. [PubMed: 2611253]

25. O'Byrne SM, Blaner WS. Retinol and retinyl esters: biochemistry and physiology. J Lipid Res. Apr 26.2013 [Epub ahead of print].
26. Wongsiriroj N, Piantedosi R, Palczewski K, Goldberg IJ, Johnston TP, Li E, Blaner WS. The molecular basis of retinoid absorption: a genetic dissection. J Biol Chem. 2008; 283:13510–13519. [PubMed: 18348983]
27. Rossant, J.; Tam, PPL. Mouse development: patterning, morphogenesis and organogenesis. Academic; San Diego: 2002.
28. Wassef L, Quadro L. Uptake of dietary retinoids at the maternal-fetal barrier: in vivo evidence for the role of lipoprotein lipase and alternative pathways. J Biol Chem. 2011; 286:32198–32207. [PubMed: 21795711]
29. Wassef L, Varsha S, Hong A, Spiegler E, Quadro L. β-carotene supplementation decreases placental transcription of LDL receptor-related protein 1 in wild-type mice and stimulates placental β-carotene uptake in a marginally vitamin A deficient mice. J Nutr. 2012; 142:1456–1462. [PubMed: 22739378]
30. Ross AC. Retinol esterification by rat liver microsomes. Evidence for a fatty acyl coenzyme A: retinol acyltransferase. J Biol Chem. 1982; 257:2453–2459. [PubMed: 7061433]
31. Yen CL, Monetti M, Burri BJ, Farese RV Jr. The triacylglycerol synthesis enzyme DGAT1 also catalyzes the synthesis of diacylglycerols, waxes, and retinyl esters. J Lipid Res. 2005; 46:1502–1511. [PubMed: 15834126]
32. Cases S, Novak S, Zheng YW, Myers HM, Lear SR, Sande E, Welch CB, Lusis AJ, Spencer TA, Krause BR, Erickson SK, Farese RV Jr. ACAT-2, a second mammalian acyl-CoA:cholesterol acyltransferase. Its cloning, expression, and characterization. J Biol Chem. 1998; 273:26755–26764. [PubMed: 9756919]
33. Goodman DS. Cholesterol ester metabolism. Physiol Rev. 1965; 45:747–839. [PubMed: 5318997]
34. Bell TA 3rd, Wilson MD, Kelley K, Sawyer JK, Rudel LL. Monounsaturated fatty acyl-coenzyme A is predictive of atherosclerosis in human apoB-100 transgenic, LDLr−/− mice. J Lipid Res. 2007; 48:1122–1131. [PubMed: 17277381]
35. Chao H, Zhou M, McIntosh A, Schroeder F, Kier AB. ACBP and cholesterol differentially alter fatty acyl CoA utilization by microsomal ACAT. J Lipid Res. 2003; 44:72–83. [PubMed: 12518025]
36. Coleman RA, Lee DP. Enzymes of triacylglycerol synthesis and their regulation. Prog Lipid Res. 2004; 43:134–176. [PubMed: 14654091]
37. Quadro L, Blaner WS, Salchow DJ, Vogel S, Piantedosi R, Gouras P, Freeman S, Cosma MP, Colantuoni V, Gottesman ME. Impaired retinal function and vitamin A availability in mice lacking retinol-binding protein. Embo J. 1999; 17:4633–4644. [PubMed: 10469643]
38. Clagett-Dame M, Knutson D. Vitamin A in reproduction and development. Nutrients. 2011; 3:385–428. [PubMed: 22254103]
39. Mark M, Ghyselinck NB, Chambon P. Function of retinoic acid receptors during embryonic development. Nucl Recept Signal. 2009; 7:e002. [PubMed: 19381305]
40. Haas D, Muenke M. Abnormal sterol metabolism in holoprosencephaly. Am J Med Genet C Semin Med Genet. 2010; 154C:102–108. [PubMed: 20104605]
41. Engelking LJ, Evers BM, Richardson JA, Goldstein JL, Brown MS, Liang G. Severe facial clefting in Insig-deficient mouse embryos caused by sterol accumulation and reversed by lovastatin. J Clin Invest. 2006; 116:2356–2365. [PubMed: 16955138]
42. Farese RV Jr, Ruland SL, Flynn LM, Stokowski RP, Young SG. Knockout of the mouse apolipoprotein B gene results in embryonic lethality in homozygotes and protection against diet-induced hypercholesterolemia in heterozygotes. Proc Natl Acad Sci U S A. 1995; 92:1774–1778. [PubMed: 7878058]
43. Farese RV Jr, Cases S, Ruland SL, Kayden HJ, Wong JS, Young SG, Hamilton RL. A novel function for apolipoprotein B: lipoprotein synthesis in the yolk sac is critical for maternal-fetal lipid transport in mice. J Lipid Res. 1996; 37:347–360. [PubMed: 9026532]
44. Willnow TE, Hilpert J, Armstrong SA, Rohlmann A, Hammer RE, Burns DK, Herz J. Defective forebrain development in mice lacking gp330/megalin. Proc Natl Acad Sci U S A. 1996; 93:8460–8464. [PubMed: 8710893]

45. Roux C, Horvath C, Dupuis R. Teratogenic action and embryo lethality of AY 9944R. Prevention by a hypercholesterolemia-provoking diet. Teratology. 1979; 19:35–38. [PubMed: 88081]
46. Zolfaghari R, Ross AC. An essential set of basic DNA response elements is required for receptor-dependent transcription of the lecithin:retinol acyltransferase (Lrat) gene. Arch Biochem Biophys. 2009; 489:1–9. [PubMed: 19665987]
47. Ziouzenkova O, Harrison EH. Retinoid and lipid metabolism. Biochim Biophys Acta. 2012; 1821:1–2. [PubMed: 22153757]
48. Ziouzenkova O, Plutzky J. Retinoid metabolism and nuclear receptor responses: New insights into coordinated regulation of the PPAR-RXR complex. FEBS Lett. 2008; 582:32–38. [PubMed: 18068127]
49. Gil-Sanchez A, Demmelmair H, Parrilla JJ, Koletzko B, Larque E. Mechanisms involved in the selective transfer of long chain polyunsaturated Fatty acids to the fetus. Front Genet. 2011; 2:57. [PubMed: 22303352]
50. Innis SM. Dietary (n-3) fatty acids and brain development. J Nutr. 2007; 137:855–859. [PubMed: 17374644]
51. Karr JE, Alexander JE, Winningham RG. Omega-3 polyunsaturated fatty acids and cognition throughout the lifespan: a review. Nutr Neurosci. 2011; 14:216–225. [PubMed: 22005286]
52. Madrazo JA, Kelly DP. The PPAR trio: regulators of myocardial energy metabolism in health and disease. J Mol Cell Cardiol. 2008; 44:968–975. [PubMed: 18462747]
53. Lefebvre P, Chinetti G, Fruchart JC, Staels B. Sorting out the roles of PPAR alpha in energy metabolism and vascular homeostasis. J Clin Invest. 2006; 116:571–580. [PubMed: 16511589]
54. Tontonoz P, Spiegelman BM. Fat and beyond: the diverse biology of PPARgamma. Annu Rev Biochem. 2008; 77:289–312. [PubMed: 18518822]
55. Kruger MC, Coetzee M, Haag M, Weiler H. Long-chain polyunsaturated fatty acids: selected mechanisms of action on bone. Prog Lipid Res. 2010; 49:438–449. [PubMed: 20600307]

Highlights

- An acyl:CoA retinol acyltransferase (ARAT) activity exists in E14.5 mouse embryo
- CMOI modulates both lecithin:retinol acyltransferase (LRAT) and ARAT activity
- Lack of embryonic CMOI results in reduced cholesteryl esters and triacylglycerols
- Lack of embryonic CMOI results in reduced mRNA levels of *LCAT, ACAT1* and *DGAT2*
- Embryonic CMOI influences esters from various substrates with multiple mechanisms

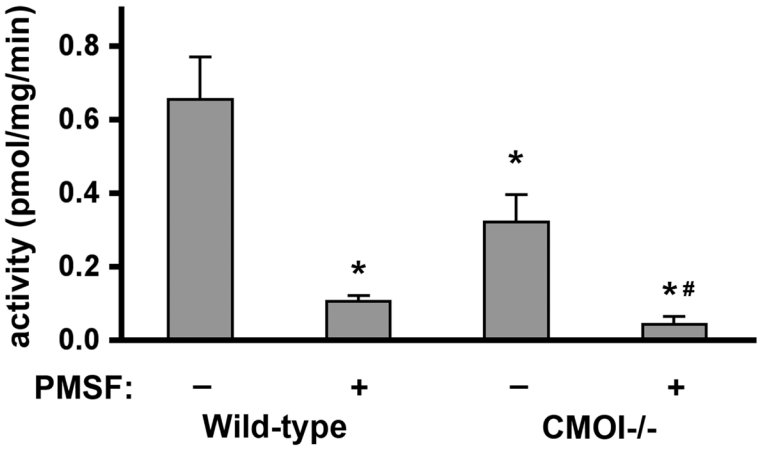

Figure 1. LRAT enzymatic activity assay

LRAT activity in microsomes isolated from wild-type and CMOI−/− embryos (14.5 dpc) from dams maintained on the vitamin A-sufficient diet throughout life and gestation. Reactions were run for 12 min at 37°C. For each genotype, 2 microsome preparations (each from 2–3 embryos from different dams) were pooled to be assayed and the experiment was repeated three times. Phenylmethanesulfonyl fluoride (PMSF) added at a final concentration of 3mM. Results are expressed as means ± SE. *P < 0.05 *vs.* wild-type *minus* PMSF; $^{\#}$P < 0.05 *vs.* wild-type *plus* PMSF.

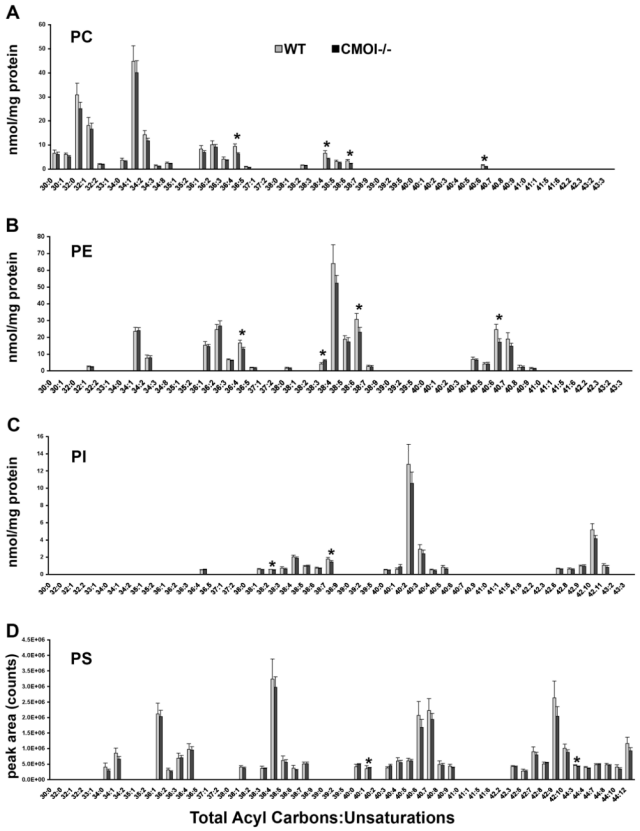

Figure 2. Phospholipid acyl chain distribution and concentrations in wild-type and CMOI−/− embryos

LC/MS analysis of phospholipids concentrations (nmol/mg protein). Values are means ± SD. *, p< 0.05, wild-type *vs.* CMOI−/− embryos by *t*-test. (**A**) PC species. Four PC species were different: PC 36:4, p <0.005, (possible fatty acid combinations: 18:2 & 18:2, 16:0 & 20:4); PC 38:4, p <0.005, (possible fatty acid combination: 18:3 & 20:1); PC 38:6, p <0.05, (possible fatty acid combination: 18:2 & 20:4); PC 40:6, p <0.05, (possible fatty acid combination: 18:0 & 22:6). (**B**) PE species. Four PE species were different: PE 36:4, p <0.01, (possible fatty acid combinations: 18:2 & 18:2, 16:0 & 20:4); PE 38:3, p <0.01, (possible fatty acid combination: 18:1 & 20:1. This is the only species that increased in CMOI−/− *vs.* wild-type embryos); PE 38:6, p <0.05, (possible fatty acid combination: 18:2 & 20:4); PE 40:6, p <0.01, (possible fatty acid combination: 18:2 & 22:6). (**C**) PI species. Two PI species were different: PI 38:2, p <0.05, (possible fatty acid combinations: 18:2 & 20:0, 18:1 & 20:1); PI 38:7, p <0.05, (possible fatty acid combination: 16:1 & 22:6). (**D**) PS species. Two PS species were different: PS 40:3, p <0.05; PS 44:3, p <0.05.

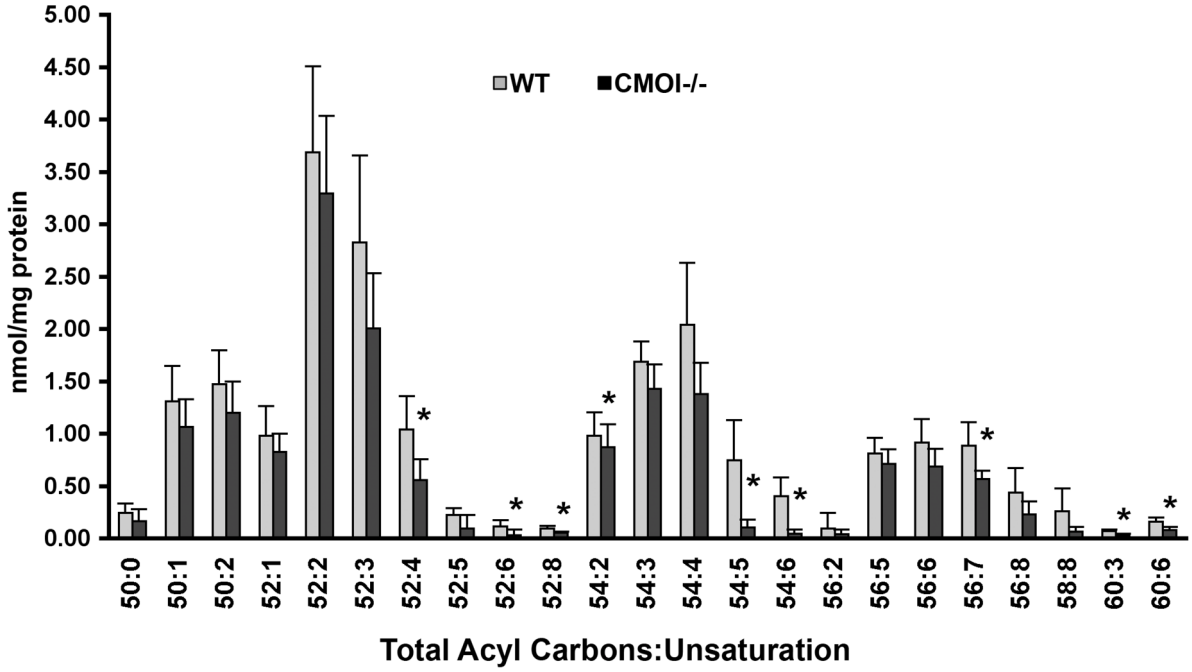

Figure 3. Triacylglycerol acyl chain distribution and concentrations in wild-type and CMOI−/− embryos

LC/MS analysis of triacylglycerol acyl chain concentrations (nmol/mg of protein). Values are means ± SD. *, p< 0.05, wild-type *vs.* CMOI−/− embryos by *t*-test.

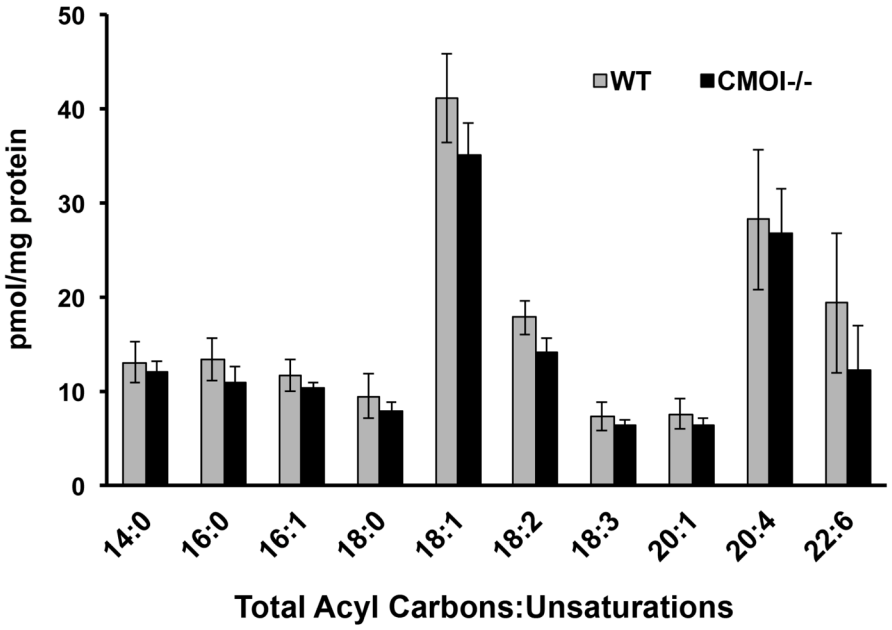

Figure 4. Fatty acyl CoA distributions and concentrations in wild-type and CMOI−/− embryos

LC/MS analysis of fatty acyl CoA concentrations (pmol/mg of protein). The experiment shown here was performed in mice fed a regular chow diet. A second experiment was performed with mice fed a purified diet containing 14 IU of vitamin A/g of diet. The results obtained from the second experiment were virtually identical to the data presented here.

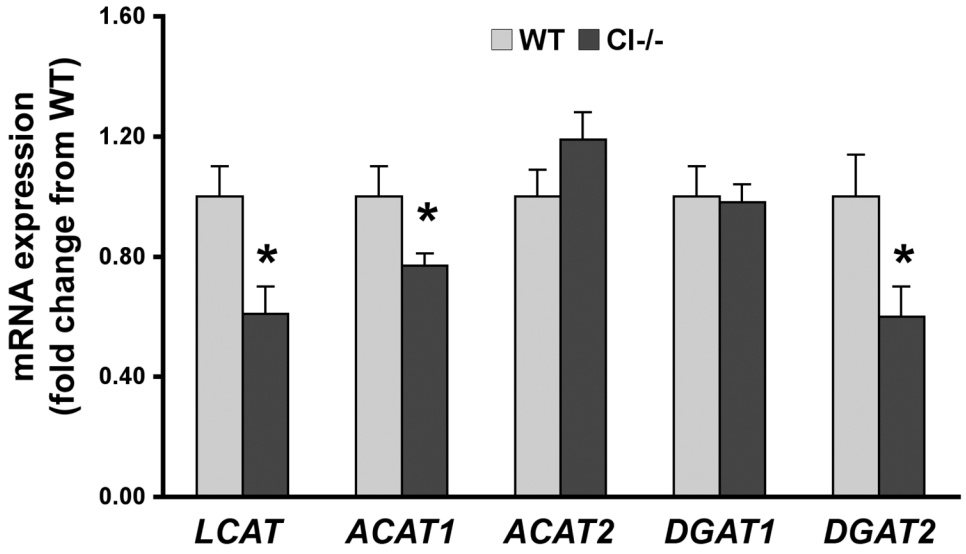

Figure 5. QPCR analysis of *LCAT, ACAT1, ACAT2, DGAT1* and *DGAT2* mRNA levels in wild-type and CMOI−/− embryos

QPCR analysis was performed as described in the Materials and Methods. Embryo wild-type (WT) set as a calibrator at 1 for each gene. Data are mean ± SD and are expressed as fold change of WT. n = 4/group. *, $p < 0.05$, wild-type *vs.* CMOI−/− embryos. The results obtained from a second experiment, performed with mice fed a purified diet containing 14 IU of vitamin A/g of diet, were virtually identical to the data presented here.

Table 1

Embryonic retinyl ester by HPLC analysis

	WT	CMOI−/−	LRAT−/−	LRAT−/−CMOI−/−
RE (ng/g)	186.5 ± 50.0	54.2 ± 18.0*	14.8 ± 7.1*	n.d.

Embryos collected at 14.5 dpc.

* $p<0.05$ vs. wild-type (WT) group. n= 4–5 embryos/genotype.

Table 2

Embryonic cholesteryl ester levels by LC/MS/APPI analysis in wild-type (WT) and CMOI−/− embryos

	nmol/mg protein	
	WT	**CMOI−/−**
O*	11.27 ± 1.95	7.73 ± 0.71 (68.8)
Po*	2.34 ± 0.60	1.25 ± 0.14 (53.5)
S*	0.90 ± 0.23	0.48 ± 0.05 (53.5)
M*	0.24 ± 0.04	0.087 ± 0.01 (36.6)
L*	2.70 ± 1.11	0.73 ± 0.09 (27.1)
P*	8.26 ± 1.61	2.18 ± 0.48 (26.4)
DHA*	0.047 ± 0.02	b.std. (<10)
Ao*	0.31 ± 0.07	0.065 ± 0.02 (21.1)
Sum of CE*,*a*	26.03 ± 3.64	12.53 ± 1.44 (48.1)

Embryos collected at 14.5 dpc.

*p<0.05 CMOI−/− *vs.* WT group. n= 4 embryos/genotype. All the values reported in this table are based on the analysis of 4.8 μg protein per each sample. The number in parenthesis indicate % of WT. b.std., the detection limit of the standard curve.

*a*values for total cholesteryl esters were calculated by adding the individual cholesteryl esters quantified. O, oleate; Po, palmitoleate; S, stearate; M, myristate; L, linoleate; P, palmitate; DHA, docosahexaenoic acid; Ao, arachidonate; CE, cholesteryl ester.

Table 3

Fatty acids in the lipid sub-classes reduced in CMOI −/− embryos

PC	% of WT	PE	% of WT	Predicted[1] Fatty Acids	Triacylglycerols	% of WT	Possible Fatty Acids	Cholesteryl Esters	% of WT
36:4	68%	36:4	78%	18:1/18:3 18:2/18:2	52:4	54%	18:2/18:2/16:0 18:3/18:1/16:0	20:4	21%
38:4	64%	38:4*	82%	20:4/18:0 20:1/18:3	52:6	24%	18:3/18:2/16:1	22:6	32%
38:6	65%	38:6	75%	20:4/18:2	52:8	60%	18:3/18:3/16:2	16:0	26%
40:6	65%	40:6	70%	22:6/18:0	54:5	14%	18:3/18:1/18:1	18:2	27%
					54:6	11%	18:3/18:2/18:1	18:0	53.5%
					56:7	64%	18:3/18:2/20:1 20:4/18:2/18:1	16:1	53.5%
					60:3	35%	20:1/20:1/20:1	18:1	69%
					60:6	52%	20:4/18:2/18:1		

[1]The fatty acids chosen were based on the fatty acyl CoA concentrations measured in embryos (Figure 4). All were significantly decreased ($p<0.05$) except PE 38:4 (*).